Liquid Crystals,
Vol. 39, No. 5, May 2012, 571–577

Taylor & Francis
Taylor & Francis Group

Alignment of the columnar liquid crystal phase of nano-DNA by confinement in channels

Dong Ki Yoon[a,b], Gregory P. Smith[a], Ethan Tsai[a], Mark Moran[c], David M. Walba[c], Tommaso Bellini[d], Ivan I. Smalyukh[a,e] and Noel A. Clark[a]*

[a]*Liquid Crystal Materials Research Center and Department of Physics, University of Colorado, Boulder, Colorado, USA;* [b]*Graduate School of Nanoscience and Technology (WCU), KINC, KAIST, Daejeon, Korea;* [c]*Liquid Crystal Materials Research Center and Department of Chemistry and Biochemistry, University of Colorado, Boulder, Colorado, USA;* [d]*Dipartimento di Chimica, Biochimica e Biotecnologie per la Medicina, Università di Milano, Milan, Italy;* [e]*Renewable and Sustainable Energy Institute, University of Colorado, Boulder, Colorado, USA*

(*Received 6 January 2012; final version received 12 February 2012*)

We demonstrate that topographic confinement in micro-channels can produce aligned domains of the columnar liquid crystal phase of complementary duplex short deoxyribonucleic acid (DNA) oligomers. Optical microscopy probing birefringence and fluorescence polarisation showed that the columnar liquid crystal phase of a 1:1 mixture of the complementary dodecamers 5′–CCTCAAAACTCC–3′ and 5′–GGAGTTTTGAGG–3′ in aqueous solution was aligned with the duplex DNA chains oriented normal to the channel axis.

Keywords: DNA; liquid crystal; columnar phase; topographic confinement

1. Introduction

The liquid crystal (LC) phase behaviour of aqueous solution of DNA has been known since the 1950s, and studied extensively by various optical and scattering methods [1–9]. These studies have revealed that duplex DNA, which in aqueous solution is a semi-flexible polymer with a 500 nm persistence length [10], is rigid enough to form bulk nematic and columnar LC phases. The generation of oriented domains of these phases has been of interest since Rosalind Franklin used shear alignment in filaments of hydrated DNA in the columnar phase to produce the x-ray diffractograms of oriented single DNA duplex strands that enabled the decipherment of the DNA duplex structure [11].

2. Results and discussion

Alignment of LC phases of DNA in solution is challenging because, at the concentration, c, required to achieve LC ordering the solutions are quite viscous. This is particularly the case with solutions of very short oligomers (nano-DNA) where nematic ordering requires 700 mg/ml $< c_N <$ 1000 mg/ml and columnar ordering requires 1000 mg/ml $< c_{CU} <$ 1500 mg/ml, with $c = 1800$ mg/ml corresponding to neat DNA [7]. LC alignment techniques can generally be categorised as mechanical (shear and flow alignment), field (electric and magnetic) and interfacial (molecular and topographic), where shear alignment is based on the anisotropic elasticity and viscosity of LCs, field alignment exploits polar ordering or dielectric or diamagnetic anisotropy, and interfacial alignment requires the interaction of LC molecules with oriented surface molecules or with induced surface modulation on scales that can range from molecular to micron. For the case of thermotropic LCs, interfacial alignment has proven to be the most useful, enabling, for example, LC display technology by the stabilisation of chosen LC cell structures in thin gaps between glass plates. In the case of DNA, shear and magnetic field have proven to be effective alignment techniques [12, 13], but interfacial alignment has not been demonstrated.

Here we report that, for the case of the LC phase of very short duplex (nano) DNA oligomers, interfacial alignment can be achieved by the topographic patterning of a silicon surface, observing that aqueous solutions of the complementary nano-DNA dodecamers 5′–CCTCAAAACTCC–3′ and 5′–GGAGTTTTGAGG–3′ produce ordered columnar phases in rectangular micro-dimension channels, both by capillary filling and by thermal cycling from the isotropic phase.

Recently, the topographic patterning of surfaces has been introduced as an effective alignment technique for LCs, based on the use of nanoimprint lithographic as well as photo lithographic techniques for generating alignment patterns [14–18]. Extending such techniques to DNA LC alignment, provides a simple new tool for producing single domain preparations for physical studies of DNA, and introduces an alignment

*Corresponding author. Email: noel.clark@colorado.edu

ISSN 0267-8292 print/ISSN 1366-5855 online

http://dx.doi.org/10.1080/02678292.2012.666809
http://www.tandfonline.com

methodology that may also be applicable to other biomaterials.

This study is motivated in part by the recent discovery of liquid crystal phases of ultra-short duplex nano-DNA and RNA oligomers [7]. Nano-length DNA oligomers, with base pair number N in the range $6 < N < 20$ have been found to exhibit both nematic (N) and uniaxial columnar (C_U) phases in aqueous solution. Such short self-complementary oligomers form double-helical duplex aggregates at room temperature which, by virtue of their hydrophobic ends, further self-assemble end-to-end to form rod-shaped superaggregates that can LC order. Both a nematic phase and a uniaxial columnar phase are found, in which the duplex stacks are on a two-dimensional hexagonal lattice, but are free to shift along the chain direction. In preparations between glass slides, in micron-sized gaps, these N and C_U phases exhibit characteristic textures, for example the conformal domain texture of the C_U phase shown in Figure 1(b), in which $\boldsymbol{n}$ is locally parallel to the plane of the glass. A variety of physical studies would benefit from the uniform in-plane alignment of $\boldsymbol{n}$, which was achieved here by topographic patterning of one of the cell substrates.

The sample studied in Figure 1 is an equimolar binary aqueous solution of the complementary DNA dodecamers A: 5′–CCTCAAAACTCC–3′ and B: 5′–GGAGTTTTGAGG–3′ (AB mixture). This solution forms double-helical duplexes generating the N phase for 700 mg/ml $< c_N <$ 1000 mg/ml and the columnar for 1000 mg/ml $< c_{CU} <$ 1500 mg/ml. The microchannels, with rectangular grooves of width $w = 3$ μm and 10 μm, separation $s = 3$ μm and 10 μm, depth, $d = 5$μm, and length, $L = 10$ mm, were prepared in the surface of single crystal Si substrates (100 orientation) by conventional fabrication techniques, including photolithographic masking and reactive ion etching (Figure 2(a)).

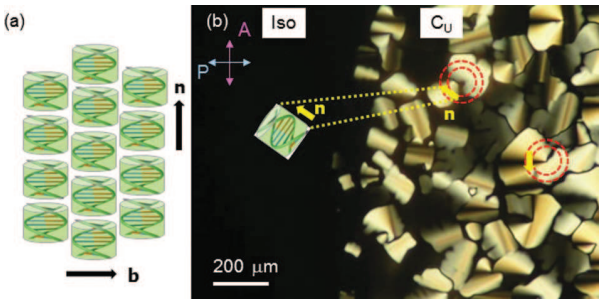

Figure 1. (a) Sketch of the duplex hydrated nano-DNA columnar LC phase. (b) Optical textures of this phase in micron-sized gaps between glass slides, obtained by depolarised transmission light microscopy (DTLM) of an equimolar AB mixture of A: 5′–CCTCAAAACTCC–3′ and B: 5′–GGAGTTTTGAGG–3′. The sketch shows nano-DNA LCs of aggregated cylindrical duplex units that have $\boldsymbol{n}$ (axis of the cylinder) and $\boldsymbol{b}$ (orientation of the base pair planes). The DTLM image shows the conformal C_U phase of the DNA LC at a concentration (1200 mg/ml) growing from the right (C_U phase) to the left (isotropic phase). The director $\boldsymbol{n}$ is shown in yellow arrows.

In order to leave a hydrophilic surface, the microchannels were thoroughly cleaned to remove organic and inorganic impurities by immersion in a mixture of dimethylformamide (DMF) and methanol, followed by rinsing several times with deionised water. The channels were then covered with a glass cover-slip, sealing around the outside of the channel area, except for a fill area, with epoxy resin in order to prevent water evaporation from the DNA solution. The resulting cell was filled with the DNA solution, putting a drop in front of the entrance described above, and letting capillarity suck the solution into the grooves (Figure 2(a)). The entrance was then sealed with epoxy resin to maintain the initial concentration of the solution during physical studies. Samples with no seal between the channel plate and glass cover were also studied (Figure 4, with width, $w = 10$ μm, separation $s = 10$ μm, depth, $d = 5$ μm, and length, $L = 10$ mm). These samples rapidly dehydrated leaving higher ordered columnar or crystal phases. In these cases the glass cover could be removed for optical study, which provided some advantages for fluorescence confocal polarising microscopy (FCPM) observation.

The resulting textures and ordering of the nano-DNA (nDNA) AB mixtures, starting from a solution with $c = 1200$ mg/ml, which is in the C_U phase at room temperature, were observed in the channels by: (i) depolarised reflected light microscopy (DRLM) to probe the optical textures and the orientation distribution of $\boldsymbol{n}$ of the C_U phase, and (ii) FCPM to investigate the three-dimensional organisation of the confined DNA LC phase. Despite the challenges presented by the extremely small DNA volume ($\sim 10^{-5}$ mm^3 for a 3 μm wide channel) available per channel, these techniques provided unambiguous evidence for the alignment of the nano-DNA C_U LC phase in the channels. Data is presented here for the $c =$ 1200 mg/ml C_U AB mixture in sealed 3 μm wide channel cells, and for the dehydrated AB mixture in uncovered 10 μm wide channels.

Because the Si substrate is opaque the optical textures of the birefringence of the channel confined solution were observed in reflection between crossed polariser and analyser (DRLM). The reflected light intensity depends on the wavelength (λ), birefringence ($\Delta \boldsymbol{n}$) and sample thickness (t) based on the equation, $I = I_0 \sin^2 2\varphi \sin^2 \frac{\pi 2t\Delta n}{\lambda}$, where φ is the angle between a principal optic axis and the polarisation direction

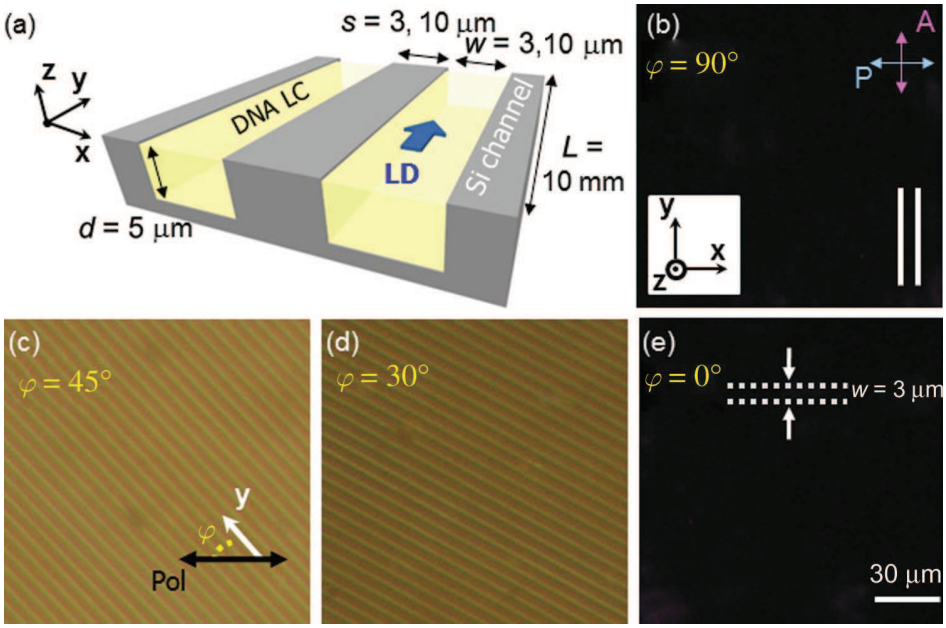

Figure 2. Sample preparation of duplex hydrated nano-DNA columnar LC phase in the confined micro-channels and optical images obtained by depolarised reflected light microscopy (DRLM). (a) LC is filled in the silicon channels with 5 μm depth and 3 μm width (or 10 μm width for the dehydrated sample of Figure 4), and the x-, y- and z-directions are defined. LD is the loading direction of the LC sample. (b–e) Optical images of the confined DNA phase in the confined area $\varphi = 90°$, 45°, 30° and 0° rotated sample respectively. Clear alternation of brightness is observed upon rotating the sample, giving information about the molecular orientation in the channel; the two parallel white bars in image (e) indicate channel direction 'y'.

(Figure 2(c)) and the path length is $2t$ for observation in reflection. We can consider two basic orientations of the C_U phase: with $\boldsymbol{n}$ normal to the plates there is no in-plane birefringence and the image is dark (see Figure S4 in reference [7]); with $\boldsymbol{n}$ parallel to the cell plates, the uniaxial birefringence $\Delta\boldsymbol{n} = \boldsymbol{n}_{||} - \boldsymbol{n}_{\perp}$, where $\boldsymbol{n}_{||}$ is the refractive index for light polarised parallel to $\boldsymbol{n}$ and $\boldsymbol{n}_{\perp}$ is the refractive index for light polarised normal to $\boldsymbol{n}$, produces a relative phase shift of these modes. The $\sin^2 2\varphi$ term in I gives minimum reflectance for $\varphi = 0°, 90°, 180°, \ldots$, and maximum intensity for $\varphi = 45°, 135°, \ldots$. This dependence produces the characteristic brush pattern of the conformal domains of the C_U phase when the columns are parallel to the plates, with the dark brushes being regions having $\boldsymbol{n}$ either parallel or normal to the polariser axis [19]. These two cases can be distinguished since in such domains the columns bend around as arcs of circles and are thus normal to the brushes. The inherent optical anisotropy of the columnar phase can be determined by measurement of the sign of $\Delta\boldsymbol{n}$, for example by putting a variable compensator in series with the cell between the polariser and analyser. In the case of the C_U phase of both nano- and long DNA, $\Delta\boldsymbol{n} < 0$, i.e. $\boldsymbol{n}_{\perp}$ is greater than $\boldsymbol{n}_{||}$, a result of the alignment of the conjugated molecular planes of the bases normal to the duplex helical axis, $\boldsymbol{n}$.

Upon cooling the AB mixture between untreated plates, the C_U phase exhibits heterogeneous nucleation and grows in from the black isotropic phase in Figure 1(b) as bright birefringent conformal domains, without any global orientation. However, with the channel topography on the Si cell surface distinct overall orientational ordering appears, as shown in Figures 2(b–e) and Figures 4(a–c) and (l–n), with minimum transmission where the angle φ between the polariser and **x**, normal to the channel direction, is $\varphi = 90°$ and 0° (Figures 2(b) and (e)). This, in turn, indicates that the C_U phase principal axis is aligned perpendicular or parallel to channel direction (**x** or **y** axis of the channel in Figure 2).

In order to further probe the DNA alignment, FCPM visualisation was carried out. The specimen must be fluorescent for such an experiment, but our DNA LC sample was not fluorescent. Thus, this sample was mixed with the dye acridine orange (Figure 3(g)), a fluorescent probe in DNA microscopy [20, 21]. Acridine orange binds strongly to duplex DNA by intercalation between successive base pairs, showing an excitation maximum at 460 nm (blue) and exhibiting red fluorescence with a maximum wavelength of 650 nm. The acridine orange dye absorption and emission dipoles are parallel to its molecular long axis, which is normal to the duplex axis $\boldsymbol{n}$ in the

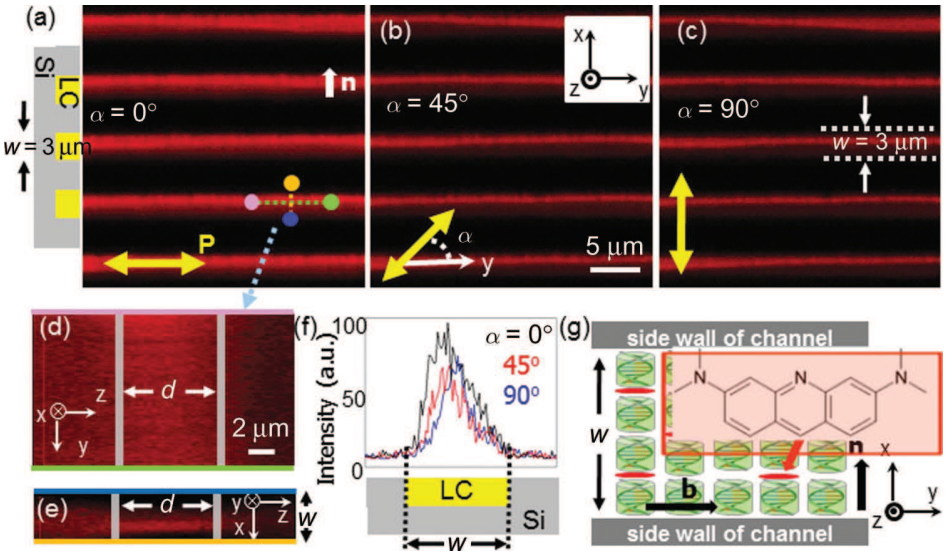

Figure 3. FCPM images of aligned duplex hydrated nano-DNA LC in $w = 3$ μm wide Si channels. (a) 0° polarisation (parallel with channel direction (y)) is used and shows the brightest signal, revealing that the planes of the acridine orange dye molecules are aligned along the channel, indicating that the DNA duplex axes are aligned perpendicular to the channel direction. The fluorescent images under (b) 45° and (c) 90° rotated polarisation light decrease in intensity. (d) The y–z plane and green and pink lines, normal to the page in (a). (e) The x–z plane in (a) shows that DNA LC is well packed in the channels. (f) Cross-section FCPM views of the dye in a single channel. The grey line is the z-range of filled DNA molecules. Averaged fluorescent signal intensity of three lines in each image that obtained during changing excitation polarisation direction (0° (black), 45° (red) and 90° (blue)). (g) A sketch of columnar nano-DNA and acridine orange dyes in the channel.

intercalated state. The resulting emissive intensity is at maximum when the excitation light is polarised normal to ***n***. With an analyser having the same orientation, the detected fluorescence intensity varies as $I \propto \cos^4\alpha$, where α is the angle between the base pair direction ***b*** (Figures 1(a) and 3(b)) and the polarisation direction of scanning laser, offering a sensitive probe for DNA orientation and ordering.

Figures 3(a–c) show FCPM images of samples of the AB nDNA mixture filled into the channels ($w = 3$ μm) by capillarity at room temperature. The fluorescence intensity was measured as a function of the angle α between the exciting polarisation direction and the **y** direction parallel to the channels (Figure 3(b)). In all cases the brightest fluorescent signal could be observed when the excitation polarisation direction was parallel with the channels ($\alpha = 0°$), showing successively darker images as α was increased to 90° (Figure 3). This dependence on α indicates that the preferred orientation of the duplex chains is normal to channel direction.

Confocal scans of fluorescence intensity averaged along the channels are shown in Figure 3(f). The dependence of the intensity on polarisation orientation means that acridine orange dye molecules are mostly aligned parallel with the channels, and the director of the C_U phase (***n***) of DNA LC molecules is oriented perpendicular to the channel as described in Figure 3(g).

Quantitative measurements of the integrated fluorescence intensity from a channel above the background level obtained between channels, shows the largest fluorescent signal for $\alpha = 0°$. Taking this value to be $I_F(0°) = 1$, we find $I_F(45°) = 0.61$ and $I_F(90°) = 0.59$ for $\alpha = 90°$, indicating an order parameter, $Q = 0.32$ for the acridine orange in the channels, as discussed below [22]. Cross-sectional views of this sample show how the molecules are filled in the confined geometries in the y–z plane (green line; from pink to green point) and the x–z plane (orange line; blue to orange point), although this does not show molecular level structure (under 5 nm) of DNA LC molecules due to the optical resolution (~100 nm) of FCPM (Figures 3(d) and (e)).

Figure 4 shows DRLM and FCPM images for the AB mixture in 10 μm wide channels. For Figures 4(a–k) uncovered channels were filled by capillarity with $c = 1{,}200$ mg/ml solution and left to dry at room temperature, while for Figures 4(l–n) the channels were covered by a glass slide and the DNA LC domains in solution were grown by temperature cycling. Scanning confocal imaging of the reflected light shows the 5 μm (d) deep channel topography and a 2.5 μm deep DNA film (t) in the channel bottom.

The white dotted lines show the channel boundaries (Figure 4(k)), while yellow ones indicate the DNA LC material (Figure 4(h)). The DRLM images, made with incandescent illumination, show an optical channel width that is larger than the actual geometry, because of diffractive broadening, whereas the FCPM images show it as narrower, because of the diffractive loss at the silicon step of the channel edge (the white arrow in Figures 4(h) and (k)). The DRLM images show significant alignment of the dehydrated DNA. The orientations with polarisation along or normal to the channel direction ($\alpha = 0°$, 90°) are dark with brighter areas indicating fluctuations and localised defects in the alignment. The white/yellow birefringence colour indicates a net retardance, $r = \sim 0.4$ μm, coming from the incident and reflected passes through the $t = 2.5$ μm deep nDNA layer, giving an average nDNA birefringence $\Delta n = r/2t \sim 0.1$. This is comparable to

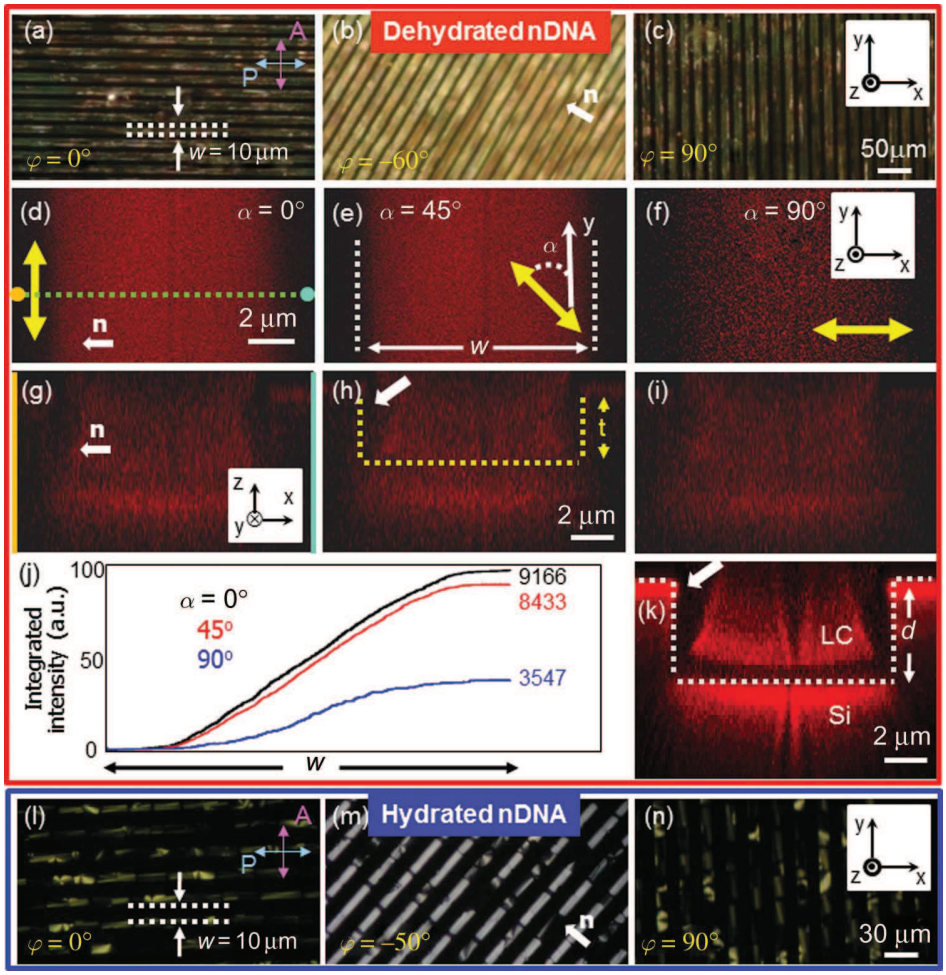

Figure 4. DRLM and FCPM images of aligned dehydrated and hydrated duplex nano-DNA (nDNA) LC in the channels. (a–c) Optical images of dehydrated nDNA columnar LC phase in the channels of $\varphi = 0°$, 45° and 90° rotated samples respectively, revealing the same orientation tendency as the hydrated DNA LC phase in the channels (Figures 2(a–c)). (d) 0° of polarised scanning laser (parallel with channel direction) is used and shows the brightest signal, indicating that dyes are aligned through the channel and that DNA LC columns are aligned perpendicular to the channel direction. (e) The fluorescent image under 45° rotated polarised scanning laser shows a dim signal relative to that of (d). (f) 90° polarisation (perpendicular to the channel direction) shows the dimmest fluorescent signal because the polarisation of the scanning laser is perpendicular to the molecular axis. (g–i) Cross-section views of the orange line (d–f) show the consistent brightness as measured in x–y plane respectively. The actual thickness, t, of the dehydrated LC sample is described by yellow dashed lines. (j) Fluorescent signal intensity of each image that was obtained whilst changing excitation polarisation direction (0° (black), 45° (red) and 90° (blue)). (k) The reflective FCPM image clearly shows each Si–LC boundary. White dashed lines indicate the boundaries of Si channels and yellow dashed lines indicate the LC; the dark area pinpointed by a white arrow indicates the optical artefact by diffractive light of high numerical aperture (NA) of FCPM. (l–n) DNA LC domains in solution grown by temperature cycling show the same tendency as the dehydrated sample upon rotation.

the neat nDNA birefringence $\Delta n \sim 0.125$, obtained by extrapolation of the birefringence of nDNA measured in the C_U phase in solution ($\Delta n \sim 0.025$ at $c = 350$ mg/ml) to the concentration of that of neat dehydrated DNA ($c = 1800$ mg/ml). The nDNA film index is larger for optical polarisation parallel to the channel, indicating a nDNA orientation like that sketched in Figure 3(g), the same preference as in the 3 μm wide channels.

The thermally cycled 10 μm wide channel samples showed the greatest promise for obtaining high quality alignment (Figures 4(l–n)), cooling into domains that nucleated on the channel side walls robustly with $\boldsymbol{n}$ normal to the side walls, generating significant lengths of channel with nearly perfect alignment, interrupted by conformal columnar defects.

In order to further probe DNA orientation we extracted order parameters from the measurements of the fluorescence depolarisation ratio $R = I(\alpha = 90°)/I(\alpha = 0°)$, averaged over the channel widths, excluding a 1 μm thick layer next to each channel wall which was not illuminated due to the diffractive loss caused by high numerical aperture (NA = 1.3) of objective lens of the FCPM. The corresponding fraction, f, of the illuminated volume with $\boldsymbol{b}$ parallel to the channel direction is then $f = 1/(1 + R)$. We found $R = 0.33, f = 0.75$ for the 10 μm channels (Figure 4(j)), and $R = 0.59, f = 0.63$ for the 3 μm channels (Figure 3(f)), indicating that the dehydrated nDNA in the wider channels has better alignment of the duplex chains normal to the channel direction.

This trend is apparently due to the preference for the DNA chains to align normal to the channel side surfaces. nDNA alignment with the chains normal to the surfaces is also seen occasionally with glass, although the predominant alignment on glass is with the chains parallel to the surface.

We also studied the effects of flow on the alignment, producing in-plane shearing of nDNA LC domains in cells made of thin glass, as well as driving flow up and down the channels. The columnar LC domains are viscous, but if the shear is strong enough they will deform under its influence and reorient with the chains along the velocity direction and normal to the shear direction. However this behaviour is not obtained from flow in the channels as the LC domains in the channels almost always flow in the channels with little deformation, apparently lubricated at the channel walls by the much lower viscosity isotropic phase. There is then little flow alignment in the channels.

3. Conclusions

The low molecular weight of the nDNA system studied here enables effective duplexing, self-assembly and LC domain formation alignment by the topography of the channels. Of particular interest for future study is the preparation of such samples for x-ray diffraction studies of the nDNA duplex structure in the LC domains.

4. Experimental details

The equimolar binary aqueous solution of the complementary DNA dodecamers A: 5′–CCTCAAAA CTCC–3′ and B: 5′–GGAGTTTTGAGG–3′ (AB mixture) was prepared as reported previously [7]. Cross-section square type of micro-channels of silicon wafers were prepared by using photolithography and reactive ion etching techniques [16, 17]. After removing organic and inorganic impurities by immersion in DMF and methanol, then rinsing several times with deionised water, these channels were filled with the DNA solution by capillary force (Figure 2(a)), followed by sealing with epoxy resin to maintain the initial concentration of the solution.

The optical anisotropic textures of samples in the channels in the C_U phase were observed under DRLM (Nikon Eclipse E400 POL) at room temperature whilst rotating the sample to determine the optical axis of the C_U phase of duplex nano-DNA LC. The polarised fluorescence signal of the C_U phase of DNA LC was investigated with a FCPM [21] based on the FV300 confocal system with an inverted microscope base IX81 (Olympus). The visible light of an Ar-laser excitation beam (488 nm) from the dye (acridine orange) doped sample exhibits a red fluorescence (650 nm). We used the oil-immersion objective (100×) lens, three-dimensional imaging and reconstructing cross-sections of DNA LCs in the micro-channels with different linear polarisations (Figures 3 and 4) using the FV1000 software (Olympus).

Acknowledgements

This was supported by MRSEC Program by NSF DMR-0820579, World Class University Program through the National Research Foundation of Korea funded by the Ministry of Education, Science and Technology (R31-2008-000-10071-0), KAIST Institute for the NanoCentury, and I2CAM Junior Exchange Award by NSF grant DMR-0645461 under ICAM-I2CAM.

References

[1] Franklin, R.E.; Gosling, R.G. *Nature* **1953**, *171*, 740–741.
[2] Wilkins, M.H.F.; Stokes, A.R.; Wilson, H.R. *Nature* **1953**, *171*, 738–740.
[3] Luzzati, V.; Nicolaieff, V.A. *J. Mol. Biol.* **1959**, *1*, 127–133.

[4] Livolant, F.; Levelut, A.M.; Doucet, J.; Benoit, J.P. *Nature* **1989**, *339*, 724–726.
[5] Merchant, K.; Rill, R.L. *Biophys. J.* **1997**, *73*, 3154–3163.
[6] Podgornik, R.; Strey, H.H.; Parsegian, V.A.; *Curr. Opin. Colloid Interface Sci.* **1998**, *3*, 534–539.
[7] Nakata, M.; Zanchetta, G.; Chapman, B.D.; Jones, C.D.; Cross, J.O.; Pindak, R.; Bellini, T.; Clark, N.A. *Science* **2007**, *318*, 1276–1279.
[8] Zanchetta, G.; Nakata, M.; Buscaglia, M.; Bellini, T.; Clark, N.A. *Proc. Natl. Acad. Sci. USA* **2008**, *105*, 1111–1117.
[9] Zanchetta, G.; Bellini, T.; Nakata, M.; Clark, N.A. *J. Am. Chem. Soc.* **2008**, *130*, 12864–12865.
[10] Hagerman, P.J. *Annu. Rev. Biophys. Biophys. Chem.* **1998**, *17*.
[11] Watson, J.D.; Crick, F.H.C. *Nature* **1953**, *171*, 737–738.
[12] Nakata, M.; Zanchetta, G.; Buscaglia, M.; Bellini, T.; Clark, N.A. *Langmuir* **2008**, *24*, 10390–10394.
[13] Kung, H.C.; Wang, K.Y.; Goljer, I.; Bolton, P.H. *J. Magn. Reson. Ser. B* **1995**, *109*.
[14] Yi, Y.; Nakata, M.; Martin, A.R.; Clark, N.A. *Appl. Phys. Lett.* **2007**, *90*, 163510.
[15] Fukuda, J.; Yoneya, M.; Yokoyama, H. *Phys. Rev. Lett.* **2007**, *98*, 187803.
[16] Yoon, D.K.; Choi, M.C.; Kim, Y.H.; Kim, M.W.; Lavrentovich, O.D.; Jung, H.-T. *Nat. Mater.* **2007**, *6*, 866–870.
[17] Yoon, D.K.; Deb, R.; Chen, D.; Körblova, E.; Shao, R.-F.; Ishikawa, K.; Rao, N.V.S.; Walba, D.M.; Smalyukh, I.I.; Clark, N.A. *Proc. Natl. Acad. Sci. USA* **2010**, *107*, 21311–21315.
[18] Yoon, D.K.; Yi, Y.; Shen, Y.; Körblova, E.; Walba, D.M.; Smalyukh, I.I.; Clark, N.A. *Adv. Mater.* **2011**, *23*, 1962–1967.
[19] Nakata, M.; Zanchetta, G.; Buscaglia, M.; Bellini, T.; Clark N.A. *Langmuir* **2008**, *24*, 10390–10394.
[20] Darzynkiewicz, Z. *Methods Cell Biol.* **1990**, *33*, 285–298.
[21] Smalyukh, I.I.; Zribi, O.V.; Butler, J.C.; Lavrentovich, O.D.; Wong, G.C.L. *Phys. Rev. Lett.* **2006**, *96*, 177801.
[22] Bellini, T.*et al.* in preparation.